Journal of Biomechanics 121 (2021) 110425

Contents lists available at ScienceDirect

Journal of Biomechanics

journal homepage: www.elsevier.com/locate/jbiomech
www.JBiomech.com

The trunk is exploited for energy transfers of maximal instep soccer kick: A power flow study

Diego da Silva Carvalho [a,b], Juliana Melo Ocarino [a,b,c], Aline de Castro Cruz [a,b], Leonardo Drumond Barsante [a,b], Breno Gonçalves Teixeira [a,b], Renan Alves Resende [a,b,c], Sérgio Teixeira Fonseca [a,b,c], Thales Rezende Souza [a,b,c,*,1]

[a] Graduate Program in Rehabilitation Sciences, Universidade Federal de Minas Gerais, Belo Horizonte, Minas Gerais, Brazil
[b] Movement Analysis Laboratory, Universidade Federal de Minas Gerais, Belo Horizonte, Minas Gerais, Brazil
[c] Department of Physical Therapy, Universidade Federal de Minas Gerais, Belo Horizonte, Minas Gerais, Brazil

ARTICLE INFO

Article history:
Accepted 25 March 2021
Available online xxxx

Keywords:
Soccer kicking
Biomechanics
Kinetic chain
Power flow
Mechanical energy

ABSTRACT

The purpose of this study was to investigate the angular kinetic energy transfers and expenditure among the trunk (bisegmented), the pelvis and the kick limb during maximal soccer instep kicking, and to characterize kicking kinetics and kinematics. Eighteen adult male amateur soccer players (24.0 ± 4.1 years old) were assessed. Three-dimensional kinematics and ground reaction force were measured. A 6-degrees-of-freedom model was assumed, comprising the upper trunk, lower trunk, pelvis, thigh, shank and foot, and the thoraco-lumbar, lumbo-pelvic, hip, knee, and ankle joints. Angular kinematics and joint moments were computed. Power flow analysis was done by calculating the joint powers (to describe joint-to-segments energy transfers) and the proximal and distal segment powers (to describe segment-to-segment transfers). Power, kinematic and kinetic time series were presented to describe the energy flows' directions. The total mechanical energy expenditure (TMEE) at each joint was also calculated. The TMEEs pointed to substantial energy expenditure at the trunk (27% of the summed work produced by the analyzed joints). In the initial phases of kicking, the trunk generates downward energy flows from the upper to the lower trunk and from the lower trunk to the pelvis, and then to the lower limb, sequentially, which favors angular motions for ball contact. There is a formation and release of a tension arc only at the hip joint, and deceleration of the segments slightly sooner than ball contact, differently from theoretical accounts. There are energy flows, hitherto unknown, among the trunk, pelvis and kick limb, revealing mechanical strategies of kicking.

1. Introduction

Soccer kicking is extensively executed during game and training situations, and its proper execution contributes to the athlete's and team's performance (Rahnama et al., 2002). In addition, several injuries have been reported as related to the mechanics of soccer kicking, such as muscle strains (Cross et al., 2013), pelvic dysfunctions/groin pain (Serner et al., 2015) and back pain (El Rassi et al., 2005). Therefore, understanding the mechanical aspects of kicking is of interest for sports professionals and researchers aiming to optimize player's performance and to comprehend potential mechanisms for musculoskeletal injuries. Studies of kicking biomechanics have focused on the kinematics, kinetics (Kellis and Katis, 2007; Lees et al., 2010a) and power flow (Robertson and Mosher, 1985) of the kicking limb. However, due to the mechanical coupling among body segments (Zajac et al., 2002), the involvement of segments and joints proximal to the lower limbs during kicking should also be understood.

Previous studies have described the kinematics of the upper body during soccer kicking. Shan and Westerhoff (2005) showed that experienced players exhibit large trunk and upper limb motion. Further, Fullenkamp et al. (2015) showed that skilled players had greater trunk axial rotation range of motion and peak trunk rotation velocity compared with novice players, and that this was associated with increased ball velocity. Such evidence suggests

* Corresponding author at: Graduate Program in Rehabilitation Sciences, Universidade Federal de Minas Gerais, Belo Horizonte, Minas Gerais, Brazil.
E-mail address: thalesrs@ufmg.br (T.R. Souza).
[1] Mailing address: Departamento de Fisioterapia - Escola de Educação Física, Fisioterapia e Terapia Ocupacional - Universidade Federal de Minas Gerais. Av. Presidente Antônio Carlos, 6627 – Campus Pampulha, Belo Horizonte – MG - CEP 31270-901, Brazil.

https://doi.org/10.1016/j.jbiomech.2021.110425
0021-9290/

that the mechanics of upper body segments, such as the trunk (including the pelvis), is relevant for kicking. In addition, theoretical accounts proposed that the trunk and the joints connecting the trunk to the kicking lower limb may be exploited to better propel the ball forward (Fonseca et al., 2011; Shan and Westerhoff, 2005). Overall, these accounts suggest mechanisms in which the moments of force exerted at the trunk occur in favor of the typical motions of the kicking limb; i.e., to accelerate the limb before ball contact and to decelerate it after contact (Fonseca et al., 2011; Shan and Westerhoff, 2005). In this sense, there could be mechanical energy storing and releasing in a hypothetical tension arc formed by the body (Shan and Westerhoff, 2005) and/or a proximal to distal transfer of mechanical energy (Fonseca et al., 2011). Unfortunately, the existing kinematic descriptions alone cannot be used to verify these kinetic and energetic suppositions. Therefore, there is a need for a description of the kinetics and energy flows among the joints and segments of the trunk and swing lower limb, in order to understand the mechanical strategies used to perform maximal instep kicking of soccer.

The present study investigated the angular kinematics and kinetics of the maximal instep kicking, including the upper trunk, lower trunk and pelvis. A power flow analysis was carried out to describe the kinetic energy transfers and expenditure among the trunk and kick lower limb segments and joints.

2. Materials and methods

2.1. Experimental design and participants

Eighteen adult male amateur soccer players (age: 24.0 ± 4.1 years, height: 1.73 ± 0.07 m, mass: 69.57 ± 10.5 kg, BMI: 22.86 ± 2.89 kg/m^2) who practiced soccer as a recreational activity at least once a week for a minimum period of one year were recruited by convenience of university soccer teams and recreational soccer clubs to participate in this cross-sectional observational study. All participants were skilled at kicking, played at a good amateur level and had at least eight years of experience playing soccer (12.9 ± 4.8 years). The test procedures of this study were approved by the institution's Research Ethics Committee (CAAE – 42162915.9.0000.5149) and the participants signed an informed consent form.

The inclusion criteria were: right foot dominance (verified with the question: "If you were to kick a ball, which foot would you kick with to achieve the maximal ball speed?"); age between 18 and 35 years; body mass index of 28 kg/m^2 or less; playing soccer as a recreational activity at least once a week for a minimum period of one year; absence of musculoskeletal injuries and/or surgery in the lower limbs, pelvis or trunk in the last 12 months; and absence of musculoskeletal symptoms in the last three months. The exclusion criteria were: presence of any discomfort during the kicking trials; drugs or alcohol consumption or engagement in any type of physical training or exercise in the 24 h prior to data collection.

2.2. Kinematic and kinetic assessment of kicking

For the kinematic assessment of kicking, the three-dimensional motion analysis system Codamotion (Charnwood Dynamics, Rothley, England) with four capture units for active markers was used, at a sampling rate of 100 Hz. To obtain kinetic data, a synchronized OR6-6 force platform (Advanced Mechanical Technology Inc. - AMTI, Watertown, USA) was used at a sampling rate of 1000 Hz.

Thirty-three active tracking markers fixed on clusters were used to track positions of nine body segments of the participants: upper trunk (thorax), lower trunk (lumbar), pelvis, thighs, legs and feet (De Leva, 1996; Iino and Kojima, 2012; Sinclair et al., 2014; Visual 3D Wiki Documentation, 2016) (Fig. 1a and b). An active tracking marker was attached to the ground, just below the ball (inside a small, 1.0×0.6 cm rectangular pit on the floor), for defining the instant the ball moved. To define a model of free rigid segments, a local three-dimensional coordinate system was created for each segment, based on the location of anatomical technical markers on specific bone prominences and virtual technical markers created in the Visual3D software (C-Motion, Inc., Rockville, USA) (Cappozzo et al.,2005) (Fig. 1c). The anatomical and virtual technical markers were also used to later define segments' dimensions and inertial properties (De Leva, 1996; Dempster, 1995; Hanavan, 1964).

Prior to data collection the participants performed a short warm-up period consisting of a maximum of 15 kicks with submaximal and maximum force, to familiarize the players with the task and the test environment. After warming up, a ten-minute rest was given.

The overview and description of the measurement setup are presented in Fig. 2 (Augustus, et al., 2017; Lees et al., 2010a). The participant was instructed to kick the soccer ball "as strong as possible" with the dorsum of the right foot (maximal instep kick), avoiding shooting the ball outside the limits of a rectangular target drawn on the canvas. The participant performed kicks until seven were considered valid for analysis. A maximum limit of fifteen kicks was established and a resting interval of one minute was given after each trial, when the participant remained seated, to avoid any muscle fatigue (Apriantono et al., 2006). All participants had seven valid trials before completing fifteen kicks.

2.3. Data processing

Kinematic and kinetic data were processed using Visual3D software. For the feet, shanks, thighs and pelvis segments, masses were estimated as percentages of total body mass, based on the Dempster's regression equations (Dempster, 1995). The location of the centers of mass, the moments of inertia and 3D dimensions of these segments were estimated according to the parameters proposed by Hanavan (1964). For the upper and lower trunks, the masses, moments of inertia, and positions of the mass centers were estimated according to the Zatsiorsky-Seluyanov's parameters adjusted by De Leva (1996). The mass of the soccer cleats was considered negligible (Nunome et al., 2002).

The tracking-markers trajectory data were filtered using a digital fourth-order, zero-lag, Butterworth low-pass filter. An optimum cut-off frequency (6 Hz) was determined by residual analysis. Force data were filtered using a fourth-order, zero lag, Butterworth low-pass filter with a cut-off frequency of 10 Hz (Winter, 2009).

2.4. Data reduction

Time series were obtained for angular motion, in degrees, of the joints and segments, in the sagittal plane. The Cardan sequence used was: mediolateral, anteroposterior and longitudinal (X, Y, Z) (Lees et al., 2010b). The kinematic and inertial data were used to calculate joint moments, in Nm, using the inverse dynamics method, with the calculation sequence beginning from the feet (Robertson et al., 2014; Winter, 2009). Joint moments were normalized by body mass (Nm/kg).

From the angular displacements and joint moments calculated, a power flow analysis was performed. The joint powers and the powers at the extremities of each segment constituting a joint (i.e., the distal power of the proximal segment (P_p) and the proximal power of the distal segment (P_d)) (watts/kg) were computed to estimate the kinetic energy changes involving the segments

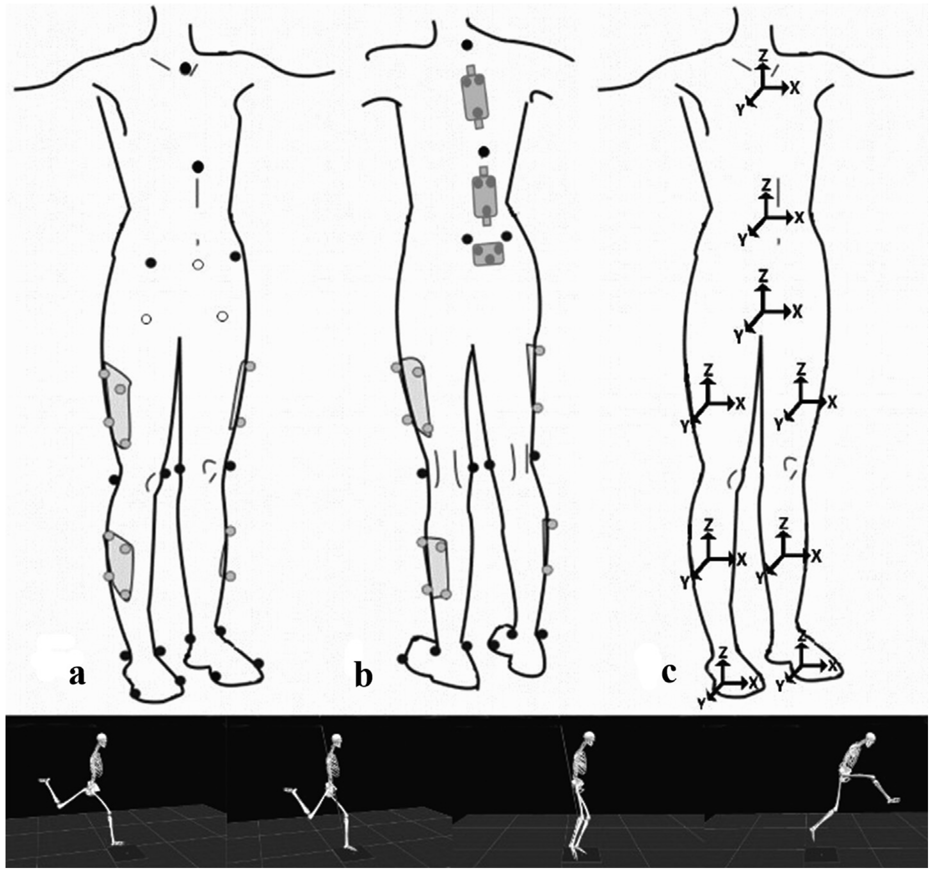

Fig. 1. Positions of anatomical and tracking markers in anterior (a) and posterior (b) views. Gray markers were used for tracking the segments. Anatomical markers (black circles) and virtual markers (white circles) were used for the definition of the biomechanical model. (c) Local coordinate systems of the feet, shanks, thighs, pelvis, lower trunk and upper trunk segments. The bottom panel illustrates the kinematics captured for one participant. Source: modified from Graci et al. (2012).

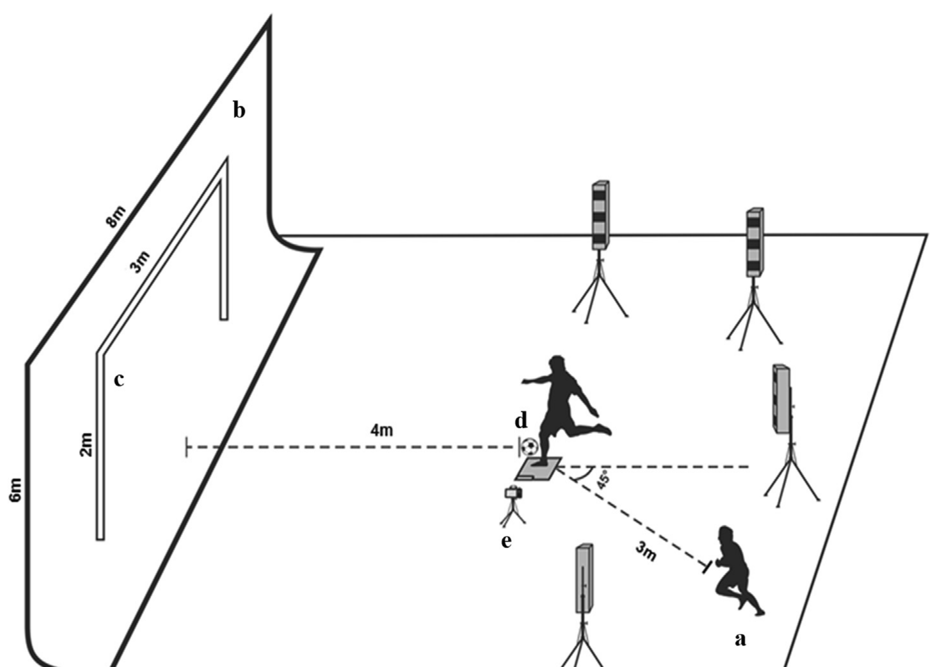

Fig. 2. Overview of the kick evaluation setup. a) initial position of the player, three meters away from the ball, in an angle of about 45° in relation to the kick direction line; b) plastic canvas (size: 8 m × 6 m), attached to the ceiling of the laboratory, at a four-meter distance from the ball, to absorb the impact of the ball; c) rectangular target drawn on the canvas with official dimensions of a futsal goal (height: 2 m; width: 3 m; thickness: 8 cm); d) position of the FIFA official soccer ball (size five, inflated at 9.0 psi) at the side of the force platform so that the support foot (i.e., left) landed on the platform; e) position of the Nikon D3100 digital camera (Nikon Inc. Tokyo, Japan) used to verify if the support foot landed within the limits of the force platform.

Table 1
Possible situations of generation, absorption and transfer of mechanical energy by the moment of force acting on a joint during kicking.

	Description of movement	Type of joint moment	Directions of segmental angular velocities	Joint function	Amount, type and direction of power
	Both segments rotating in opposite directions				
Situation 1	**Joint angle decreasing**	Concentric	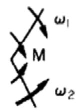	Mechanical energy generation	Mω_1 generated to segment 1. Mω_2 generated to segment 2.
Situation 2	**Joint angle increasing**	Eccentric	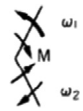	Mechanical energy absorption	Mω_1 absorbed to segment 1. Mω_2 absorbed to segment 2.
	Both segments rotating in same direction				
Situation 3	**Joint angle decreasing (e.g. $\omega_1 > \omega_2$)**	Concentric	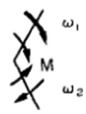	Mechanical energy generation and transfer	M(ω_1 - ω_2) generated to segment 1. Mω_2 transferred to segment 1 from 2.
Situation 4	**Joint angle increasing (e.g. $\omega_2 > \omega_1$)**	Eccentric	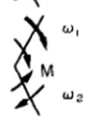	Mechanical energy absorption and transfer	M(ω_2 - ω_1) absorbed from segment 2. Mω_1 transferred to segment 1 from 2.
Situation 5	**Joint angle constant ($\omega_1 = \omega_2$)**	Isometric (dynamic)	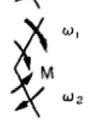	Mechanical energy transfer	Mω_2 transferred from segment 2 to 1..

M = is the joint moment; ω_1 = is the angular velocity of the segment 1 of the joint; ω_2 = is the angular velocity of the segment 2 of the joint. Source: modified from Robertson and Winter, 1980.

and their respective joints (McGibbon and Krebs, 2001; Novak et al., 2015; Robertson and Winter, 1980). The joint powers characterize joint-to-segments energy transfers and the proximal and distal powers characterize segment-to-segment transfers. These powers were expressed as follows (Novak et al., 2011, van der Krug et al., 2018):

$$P_j = M_j(w_p - w_d) = P_p + P_d = M_{jp}w_p + M_{jd}w_d$$

where P_j is the joint power; M_j is the joint moment; w_p is the angular velocity of the proximal segment of the joint; w_d is the angular velocity of the distal segment of the joint; P_p is the proximal power (i.e., distal power of the proximal segment of the joint); P_d is the distal power (i.e., proximal power of the distal segment of the joint); M_{jp} is the joint moment acting on the proximal segment; M_{jd} is the joint moment acting on the distal segment.

Following the approach of Robertson and Winter (1980), the directions of the power flows were interpreted in terms of five possible situations of transfer: (1) concentric with no transfer (generation by the joint to the segments), (2) eccentric with no transfer (absorption by the joint from the segments), (3) concentric energy transfer (transfer between segments plus generation by the joint to the segments), (4) eccentric energy transfer (transfer between segments plus absorption by the joint from the segments), (5) nearly isometric energy transfer (transfer between segments with very small generation or absorption by the joint) (Table 1).

Total mechanical energy expenditure (TMEE) was computed to characterize the total amount of energy produced/absorbed/transferred by means of the anatomical structures producing the net moment at a joint. The method described by McGibbon et al. (2001) was used. However, instead of reporting separated values of mechanical energy expenditure for the situations of concentric transfer, eccentric transfer, and no transfer, the expenditures of these situations within the kick cycle were summed up to obtain a single total value, in J/kg. The energy expenditure definition (McGibbon et al., 2001; McGibbon and Krebs, 2001) considers segment-to-segment energy transfers made by the joint, which is different from the traditionally used joint work which considers only the energy absorbed or generated by the joint (Robertson and Winter, 1980). Thus, it avoids, for example, considering the energy expenditure at a given joint as zero, in a situation in which the joint power and work are zero, but this joint is transferring energy between the adjacent segments (McGibbon et al., 2001; McGibbon and Krebs, 2001).

To facilitate interpretation of the results, the kick cycle was divided into four phases (backswing, leg cocking, leg acceleration and follow-through) according to specific kinematic events, as described by Nunome et al. (2002) and Brophy et al. (2007). All

Fig. 3. Average curves and standard deviations of the segment and joint angles, joint moments, and proximal, distal and joint powers of the thoraco-lumbar and lumbo-pelvic joints at the trunk and hip, knee and ankle joints of the kicking limb, during kicking. For the angles and powers, the blue, red and black lines correspond to the proximal and distal segments and to the joint, respectively. The dashed vertical lines on the graphs represent the limits of the phases: backswing, leg cocking, leg acceleration, and follow-through. The vertical gray bar represents the instants near ball contact, named "ball impact interval", which were not analyzed in this study. The horizontal solid bars at the top of the power graphs represent the mechanical energy transfer conditions: dark yellow indicates a concentric condition with no transfer (generation by the joint to the segments); light yellow indicates a concentric energy transfer condition (transfer between segments plus generation by the joint to the segments); dark green indicates an eccentric condition with no transfer (absorption by the joint from the segments); light green indicates an eccentric energy transfer condition (transfer between segments plus absorption by the joint from the segments); black indicates a nearly isometric energy transfer (transfer between segments). The arrows indicate the direction of the mechanical energy flow between the adjacent segments of the joint: upwards arrows show transfer to the proximal segment; downwards arrows show transfer to the distal segment; bidirectional outwards arrows show energy generation for the proximal and distal segments; bidirectional inwards arrows show energy absorption of the proximal and distal segments. (For interpretation of the references to color in this figure legend, the reader is referred to the web version of this article.)

time-series data, from all trials, were interpolated and transformed in curves with 101 points (0–100%). Kicking cycle, phases' definitions and duration, as well as a reliability analysis of the kinematic curves, are presented in supplementary material.

2.5. Descriptive analysis

Average curves from all trials and participants were generated to characterize the kinematics, kinetics and energy transfers

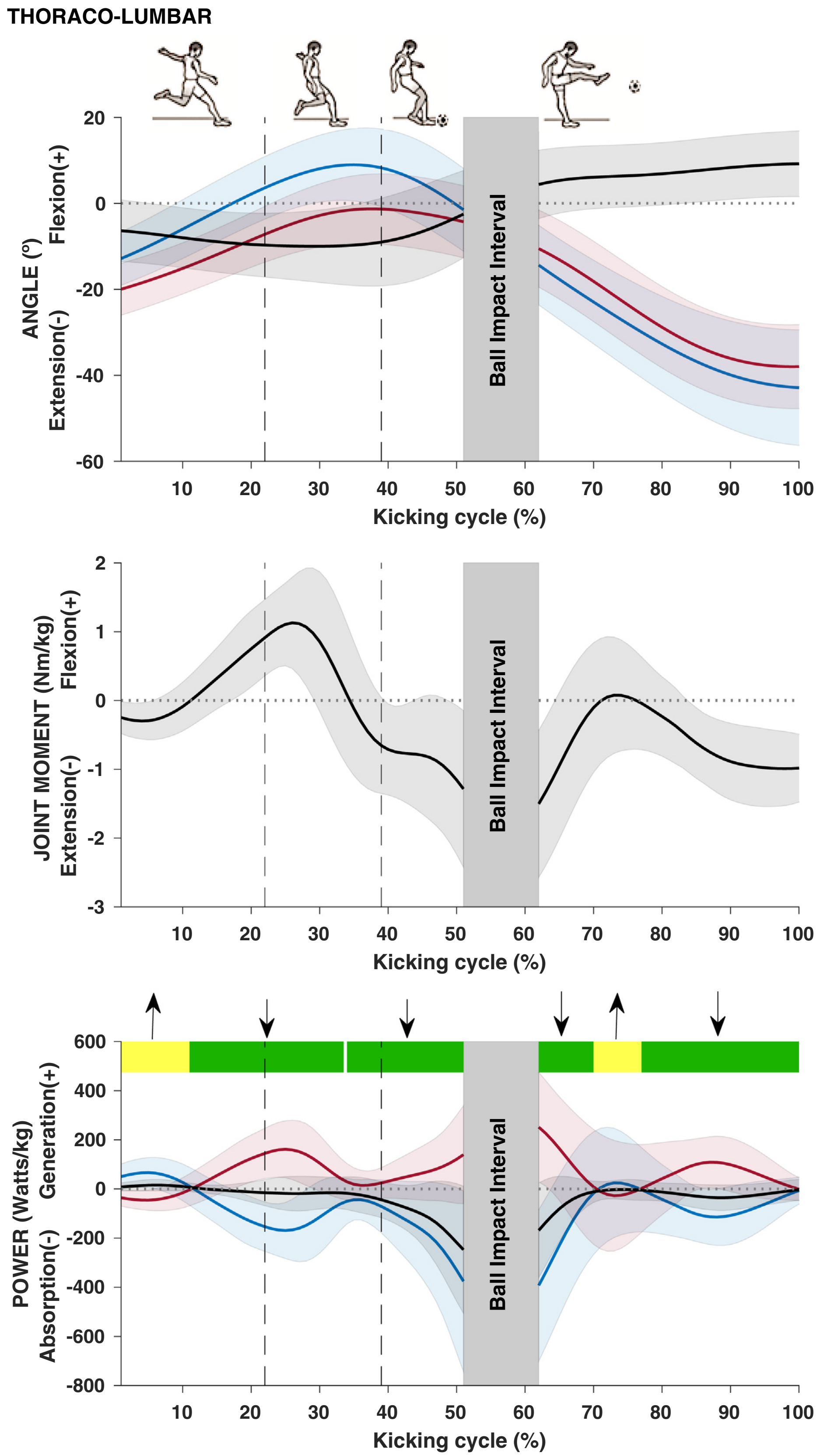

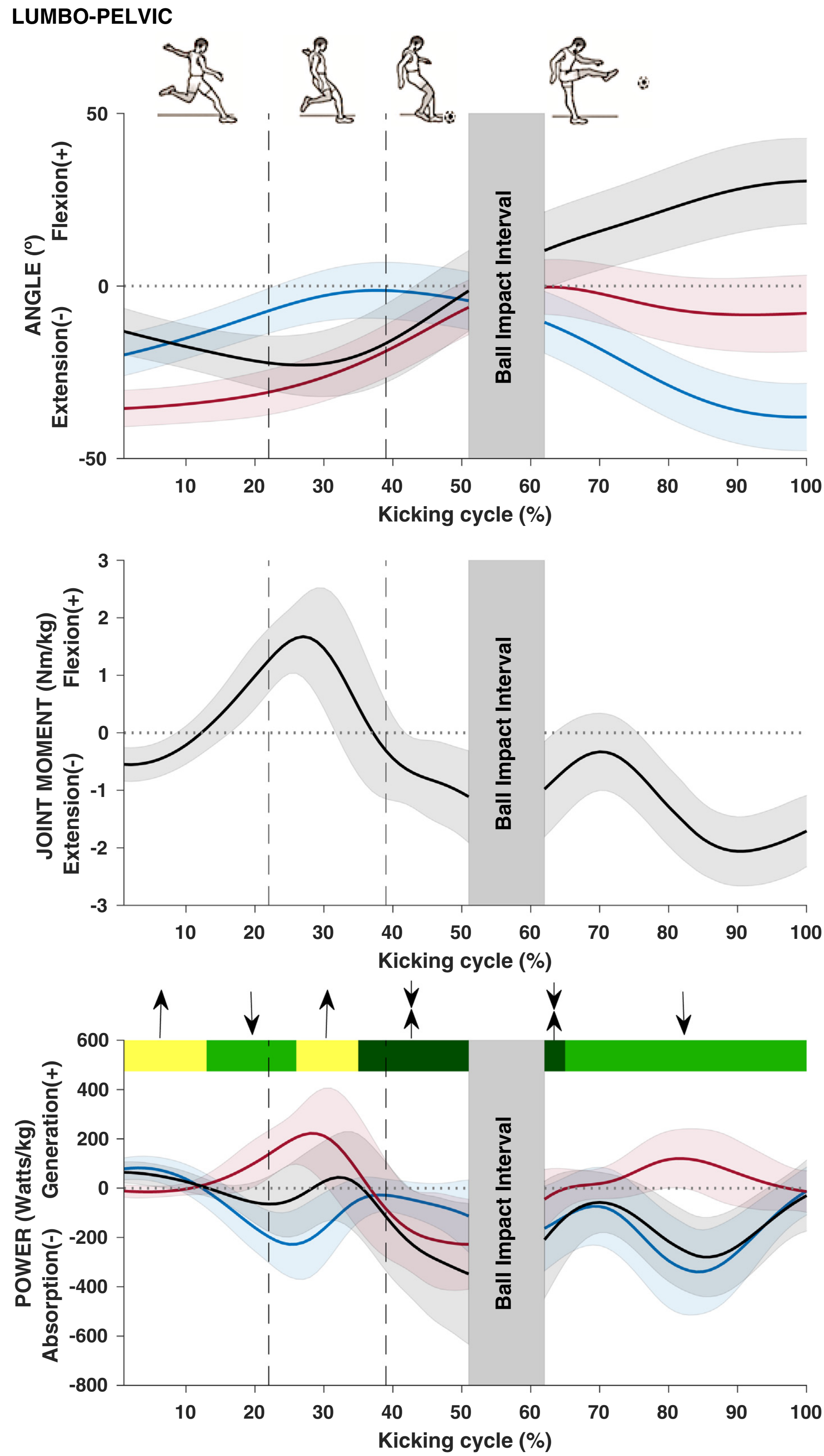

Fig. 3 (*continued*)

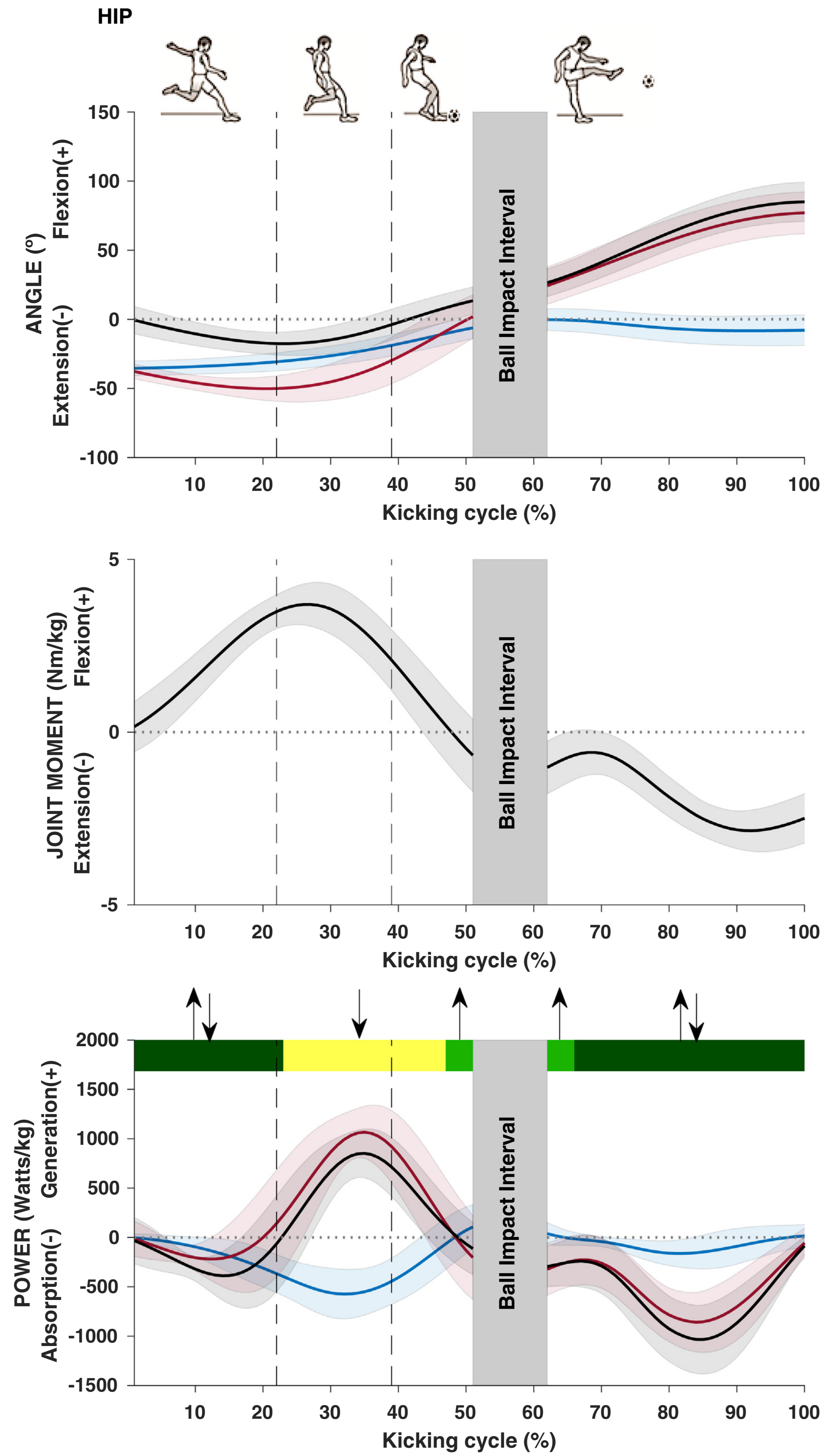

Fig. 3 (*continued*)

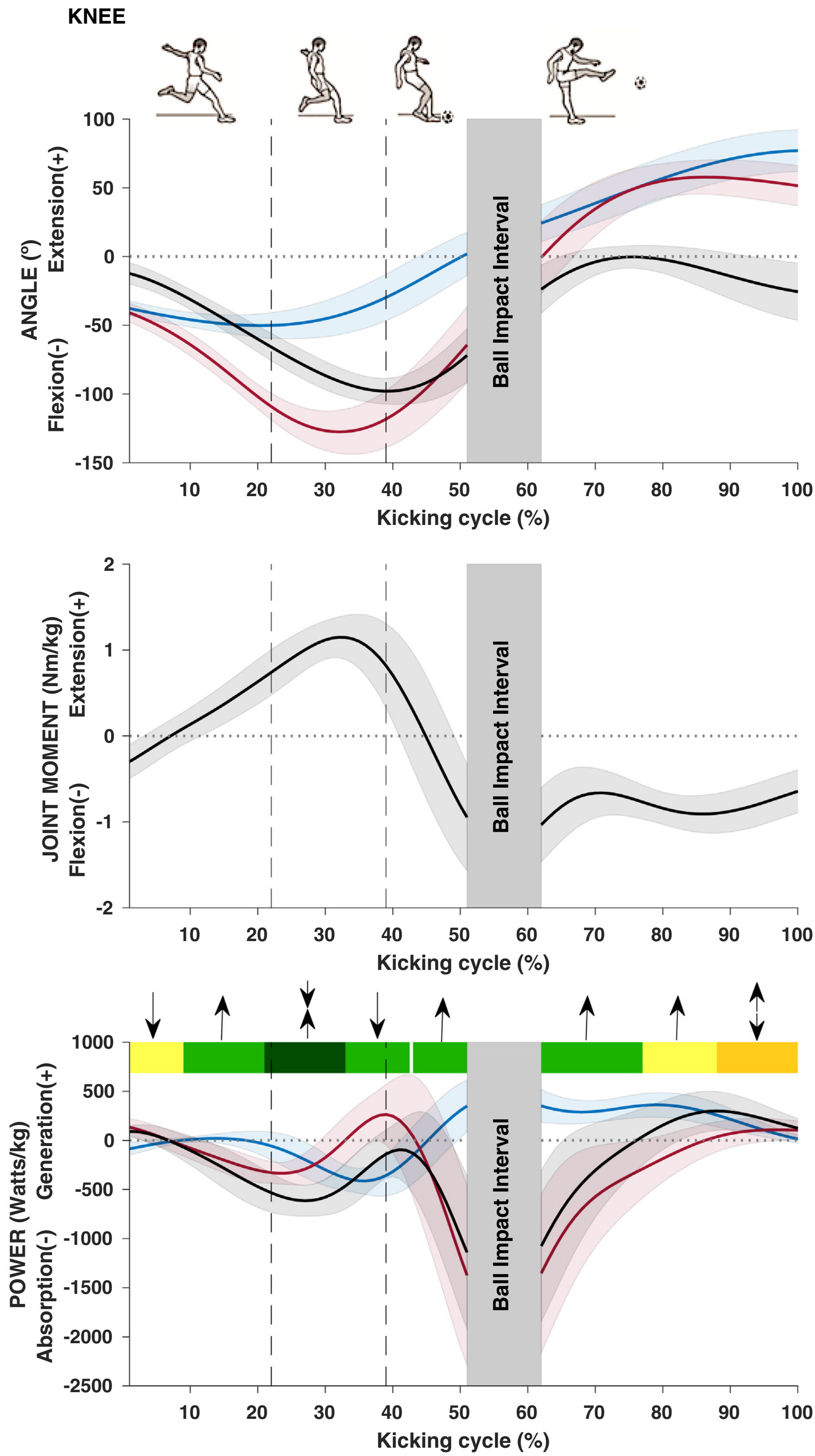

Fig. 3 (*continued*)

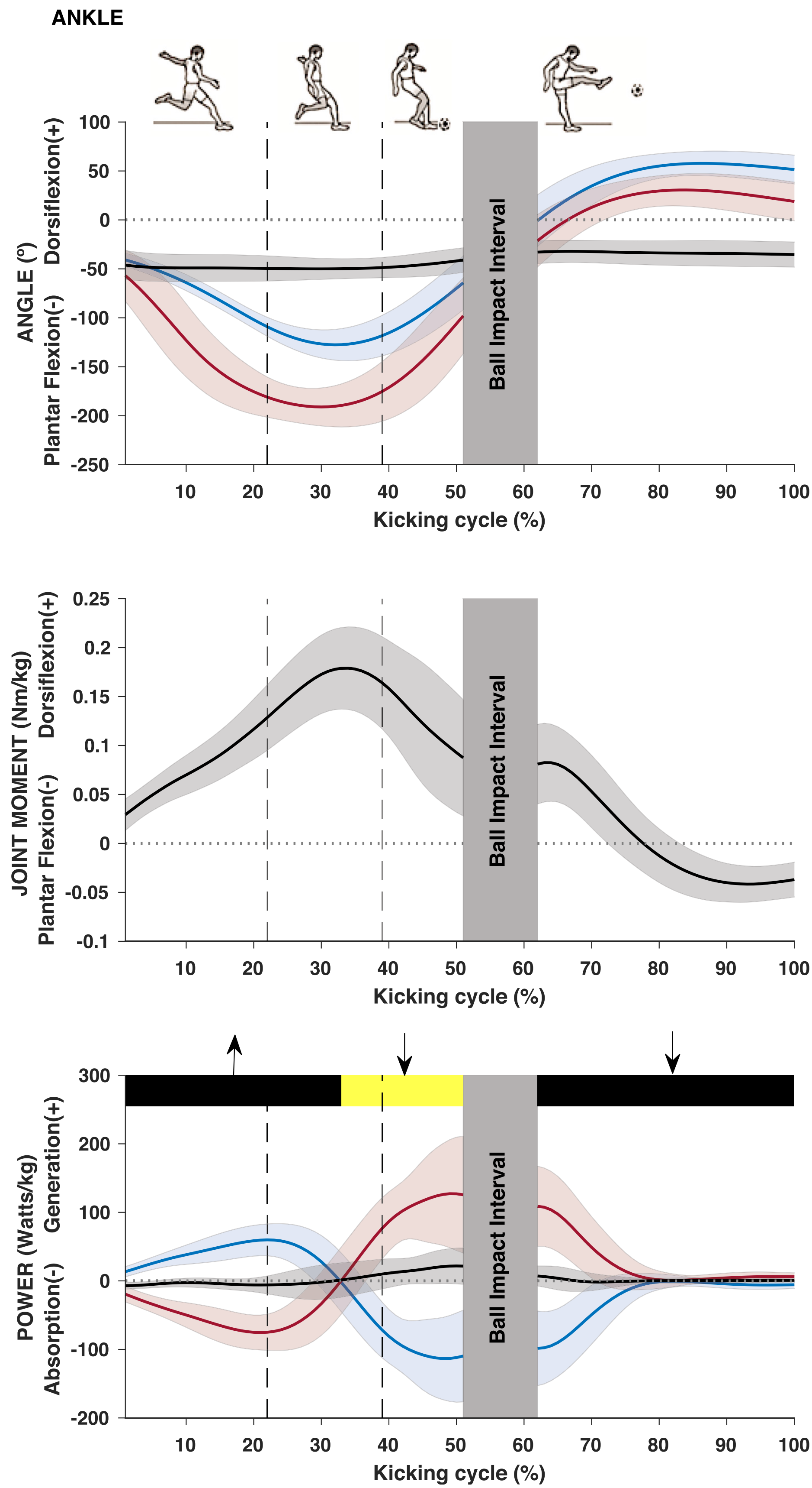

Fig. 3 (*continued*)

(powers). The events' timings, in percent of the cycle, were also averaged, to represent the phases' boundaries in the average curves. For the joints' TMEEs, means, standard deviations and ranges were calculated. Each joint TMEE was also converted into percentage of the summed TMEEs of all the analyzed joints. The means, standard deviations and ranges for the TMEEs in percentage were also calculated.

3. Results

The curves of the average segmental and joint angles, joint moments and power values showing the joint-to-segment (joint power) and the segment-to-segment (proximal and distal powers) energy transfers, during kick, are presented in Fig. 3. It can be observed that situations with segment-to-segment transfers (i.e., concentric, eccentric and isometric transfers) were predominant, which are represented by proximal and distal powers clearly different from zero and by the light green, light yellow and black horizontal bars, in Fig. 3. From the power curves and their relationship with kinematics and moments (Table 1), the directions of the energy flows among the joints and adjacent segments (arrows in Fig. 3) were revealed. Fig. 4 summarizes the predominant directions of energy flows in each phase of kicking. Predominance of power flows were verified for each kick phase and most of them were statistically significant (supplementary material). The flow directions will be further described and interpreted in terms of mechanical strategies for producing the angular motions of kicking, in the discussion section. In addition, the TMEE of the joints are presented in Table 2.

Table 2
Means, standard deviations, ranges and percentages of the total mechanical energy expenditures (TMEE) of the joints.

Joints	TMEE (J/kg) Mean (SD) [Range]	TMEE in percent of the analyzed joints (%) Mean (SD) [Range]
Thoraco-lumbar	94.64 (26.51) [53.00–173.71]	12.91 (2.66) [7.93–17.83]
Lumbo-pelvic	102.95 (21.64) [59.04–144.37]	14.06 (2.00) [8.84–18.17]
Hip	251.78 (39.34) [178.72–352.59]	34.53 (3.07) [30.08–40.15]
Knee	254.95 (33.55) [198.39–322.67]	35.09 (3.52) [29.12–43.39]
Ankle	24.63 (5.56) [16.15–36.24]	3.41 (0.83) [2.05–5.24]

TMEE = total mechanical energy expenditure; SD = standard deviation.

4. Discussion

The present study estimated and described flows of mechanical energy among segments and joints, caused by the joint moments of force of the trunk (modeled as a bisegmented trunk) and kicking limb, in the sagittal plane, during the performance of a maximal instep kicking. The patterns of the joint kinematics, moments and power of the kicking limb were similar to previous studies (Nunome et al., 2002; Robertson and Mosher, 1985; Shan and Westerhoff, 2005). To the extent of our knowledge, segmented trunk kinematics, kinetics and energy transfers (joint, proximal, and distal powers), and kicking limb segment-to-segment transfers (proximal and distal powers) have never been reported before. The data presented in Figs. 3 and 4 show that there are specific and predominant (table in supplementary material) energy transfers between the upper and lower trunks and between the lower trunk and pelvis. The observed joint TMEEs and their description in percent of the summed TMEEs of the joints analyzed point to substantial energy expenditure at the trunk segments and joints (a total of 27% for the trunk) (Table 2). The results, including the kicking limb, can be used to understand the mechanical participation of the trunk and lower limb segments and joints in producing the angular motions of kicking.

One aim of biomechanical analyses of kicking is to understand how the motions of the kicking limb can be powered to improve energy transfer to the ball, i.e., how kinetic energy arrives at the limb segments in the production of their angular motions towards the ball. Fig. 3 shows that, before ball contact, there are temporal windows at each joint with positive power values for the distal segment and negative power values for the proximal segment, which constitutes a downward energy transfer. Within these temporal windows, both adjacent segments of a joint are tilting backwards, and an eccentric or concentric (downward) energy transfer is happening. Thus, the upper segment "pulls" the lower segment to accelerate its backward rotation, by means of the joint moment (Fig. 5). Specifically, during backswing and leg-cocking phases, the curves of proximal and distal powers indicate an initial energy flow from the upper trunk to the lower trunk and a predominant flow from the lower trunk to the pelvis (Figs. 3 and 4). While there are extensions of the upper and lower trunks, retroversion of the pelvis, and extensions of the thoraco-lumbar and lumbo-pelvic joints, there are also flexion moments at both joints. However, little energy is produced or absorbed by these joints. The moments at these joints were mainly responsible for the observed energy flows from the upper to the lower segments. This rationale is supported by the low values of joint power compared to the proximal and distal segment powers, and by observing the directions (signs) of the proximal and distal powers (i.e., positive values for the distal segment and negative values for the proximal segment) (Fig. 3).

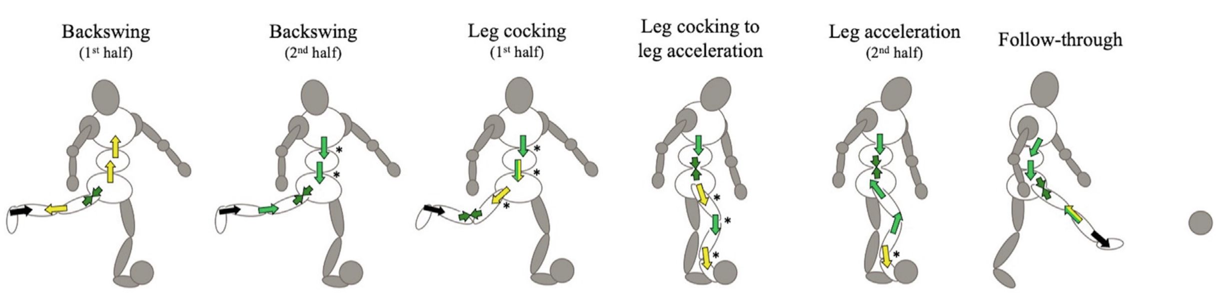

Fig. 4. Illustration of the mechanical energy flows during the kick cycle. The arrows represent the directions and conditions (concentric or eccentric) of energy transfers. The unidirectional arrows in yellow color indicate a concentric transfer of energy from one segment to another by means of the joint; the unidirectional arrows in light green color indicate an eccentric transfer of energy from one segment to another through the joint; the bicolor arrows (light green and yellow) indicate a consecutive eccentric and concentric transfer; the unidirectional arrows in black color indicate a nearly isometric energy transfer; and the bidirectional arrows in dark green color indicate an eccentric transfer of energy from the adjacent segments to the joint. The asterisks highlight downward flows of energy. (For interpretation of the references to color in this figure legend, the reader is referred to the web version of this article.)

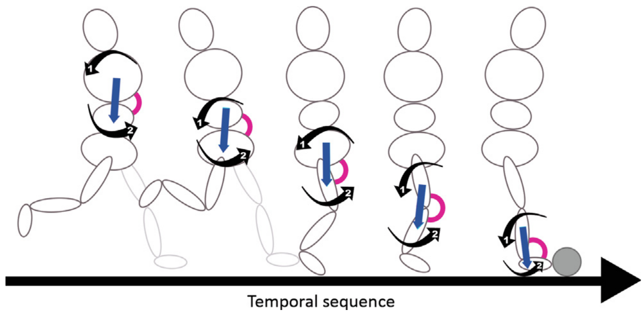

Fig. 5. Illustration of the backward rotations of the segments (black curved arrows) from the beginning of the kick until ball contact in a temporal sequence beginning from the upper to the lower segments and joints. Backward rotation of a distal segment (arrow 2) is favored by the backward rotation of its proximal segment (arrow 1) associated with the flexor moments at the thoraco-lumbar, lumbo-pelvic and hip joints, the extension moment at the knee, and the dorsiflexor moment at the ankle (joint moments are represented by the arcs in magenta color). The downward energy flows produced (straight arrows in cyan color) correspond to the production of the distal segments' backward rotations, which leads the kicking limb towards the ball. The black straight and horizontal arrow at the bottom represents the temporal sequence of kicking, before ball contact. (For interpretation of the references to color in this figure legend, the reader is referred to the web version of this article.)

The pelvis and the kicking limb presented similar behavior. During most of backswing and leg cocking phases, the pelvis was accelerated into retroversion with energy income (shown by its positive proximal power) from the lower trunk (Fig. 3). Specifically during leg cocking, the pelvic retroversion, accelerated by the interaction with the trunk, is critical for the hip flexion moment to transfer energy from the pelvis to the thigh, to accelerate it into flexion (in addition to the energy put to the thigh by the hip concentric flexion moment) (Fig. 3). Accordingly, thigh flexion is critical for the knee extension moment to transfer energy to the shank, to accelerate it into extension, at the end of leg cocking and beginning of leg acceleration phases. Finally, shank extension is crucial for the ankle dorsiflexion moment to transfer energy from the shank to the foot, to accelerate it into dorsiflexion, from the end of leg cocking until ball contact, approximately (Fig. 3). The downward energy flows show a temporal sequence beginning at the upper trunk and ending at the kicking foot, which may help the foot to demonstrate the highest angular velocity at ball contact (Fig. 5). This sequence can be noticed by observing the first positive peak of the proximal power at each joint, which occurs initially at the thoraco-lumbar joint and lastly at the ankle joint (Fig. 3). Therefore, this chain of events suggests that trunk segments and joints, in the initial phases of kicking, are exploited in energy flows that favor the lower limb angular motions towards the ball.

Theoretical accounts of kicking biomechanics suggest, based on whole-body kinematics, that during backswing the body forms a tension arc (composed of the arm of the non-kicking side, the trunk, and kicking limb) that is released at the beginning of the leg cocking phase, which would influence kick power (Fonseca et al., 2011; Shan and Westerhoff, 2005). However, by the present results, only the hip showed an early energy absorption (negative joint power during joint extension and an eccentric flexion moment) and a subsequent large energy release (positive power during joint flexion and a concentric flexion moment) (Fig. 3). Despite that, all the joints presented moments that resulted in proximal and distal powers showing downward energy flow. Therefore, the initial energy addition to the kicking limb and its angular acceleration appears to be, in great part, a consequence of the suggested backward pull made by the upper segments on the lower segments, instead of a result of a proposed elastic release of a tension arc.

Angular deceleration of the body segments started sooner than the ball contact, as opposed to what is expected in the theoretical accounts (Fonseca et al., 2010; Shan and Westerhoff, 2005). From the end of leg cocking (for the trunk) and second half of leg acceleration (for the hip and knee), the joint power curves indicated predominant energy absorption by these joints, due to the eccentric moments observed (Fig. 3). The moment at the thoraco-lumbar joint also caused an energy flow from the upper trunk to the lower trunk. Therefore, while there were forward tilts of the upper and lower trunks (trunk flexion) and the pelvis was still retroverting with flexion of the thoraco-lumbar and lumbo-pelvic joints, the upper trunk was decelerated by the thoraco-lumbar extension moment and the lower trunk and pelvis were also decelerated by the lumbo-pelvic extension moment (Fig. 3). In the kicking limb, proximal and distal powers showed an upward energy flow that helped to decelerate the distal segments. There was an initial energy transfer from the thigh to the pelvis and then a hip energy absorption from both the pelvis and thigh. There was also energy transfer from the shank to the thigh (Fig. 3). Thus, just before ball contact, the joints were already resisting the segments' angular motions by means of eccentric moments. This was different only for the ankle joint, in which there was minimal joint motion, as assumed by other authors (Dörge et al., 2002; Putnam, 1991), and a virtually isometric moment that transfers energy from the shank to the foot near ball contact (Fig. 3).

Other theoretical and practical implications can be drawn from our findings, especially for the trunk. We noticed during the first half of backswing, for instance, that initial trunk extension was partly produced by the body. There was a concentric extension moment at the lumbo-pelvic joint, with an input of energy to the lower trunk, which was partly transferred to the upper trunk by the eccentric moment at the extending thoraco-lumbar joint (Fig. 3). This initial active trunk extension suggests that the body optimizes the advantageous use of the trunk, which is consistent with the findings of greater trunk extension in experienced and skilled players than in novice players (Shan and Westerhoff, 2005). In addition, there were great mechanical demands at the trunk joints, which is shown by the large moments with magnitudes comparable to the knee joint, by the energy absorptions whose peaks reached approximately 30% of the peaks at the hip, and by the TMEE of 27% when considering the summed TMEEs at the analyzed joints (Table 2). These large demands at the trunk may be related to the relatively high incidence of low-back pain and dysfunction in soccer players (Tojima and Torii, 2018). The present findings also point to the importance of considering the motions and muscular function of the trunk to practical approaches focused on improving kicking performance (Prieske et al., 2016).

A limitation of this study is the relative low sampling rate (100 Hz) of the kinematic analysis compared to previous studies (Nunome et al., 2002; Nunome et al., 2006), which was due to the large number of active markers needed. However, the moment and power curves obtained are significantly similar to previous ones obtained with higher sampling rate (240 Hz) (Lees and Rahnama, 2013). In addition, although we excluded from our analysis all the data from a wide time interval around ball impact, the remaining data near this interval (e.g., the negative joint powers at the hip and knee just before impact) may still have been subjected to some distortion and should be considered with caution (Nunome et al., 2006).

Declaration of Competing Interest

The authors declare that they have no known competing financial interests or personal relationships that could have appeared to influence the work reported in this paper.

Acknowledgements

The authors thank the Brazilian agencies Conselho Nacional de Desenvolvimento Científico e Tecnológico (CNPq - 302887/2009-1) and Fundação de Amparo à Pesquisa do Estado de Minas Gerais (FAPEMIG - APQ-02250-15) for financial support and for a scholarship awarded to the first author (FAPEMIG). This study was financed in part by the Coordenação de Aperfeiçoamento de Pessoal de Nível Superior - Brasil (CAPES - Finance Code 001).

Appendix A. Supplementary material

Supplementary data to this article can be found online at https://doi.org/10.1016/j.jbiomech.2021.110425.

References

Apriantono, T., Nunome, H., Ikegami, Y., Sano, S., 2006. The effect of muscle fatigue on instep kicking kinetics and kinematics in association football. J. Sports Sci. 24 (9), 951–960.
Augustus, S., Mundy, P., Smith, N., 2017. Support leg action can contribute to maximal instep soccer kick performance: an intervention study. J. Sports Sci. 5 (1), 89–98.
Brophy, R.H., Backus, S.I., Pansy, B.S., Lyman, S., Williams, R.J., 2007. Lower extremity muscle activation and alignment during the soccer instep and side-foot kicks. J. Orthop. Sports Phys. Ther. 37 (5), 260–368.
Cappozzo, A., Della Croce, U., Leardini, A., Chiari, L., 2005. Human movement analysis using stereophotogrammetry. Part 1: theoretical background. Gait Post. 21 (2), 226–237.
Cross, K.M., Gurka, K.K., Saliba, S., Conaway, M., Hertel, J., 2013. Comparison of hamstring strain injury rates between male and female intercollegiate soccer athletes. American J. Sports Med. 41 (4), 742–748.
De Leva, P., 1996. Adjustments to Zatsiorsky–Seluyanov's segment inertia parameters. J. Biomech. 29 (9), 1223–1230.
Dempster, W.T., 1995. Space requirements of the seated operator geometrical, kinematic, and mechanical aspects of the body with special reference to the limbs. Michigan State University, East Lansing, pp. 1–254.
Dörge, H.C., Anderson, T.B., Sørensen, H., Simonsen, E.B., 2002. Biomechanical differences in soccer kicking with the preferred and the non-preferred leg. J. Sports Sci. 20 (4), 293–299.
El Rassi, G., Takemitsu, M., Woratanarat, P., Shah, S.A., 2005. Lumbar spondylolysis in pediatric and adolescent soccer players. American J. Sports Med. 33 (11), 1688–1693.
Fonseca, S.T., Souza, T.R., Ocarino, J.M., Gonçalves, G.P., Bittencourt, N.F., 2011. Applied biomechanics of soccer. In: Magee, D.J., Manske, R.C., Zachazewsky, J.E., Quillen, W.S. (Eds.), Athletic and Sports Issues in Musculoskeletal Rehabilitation. Saunders Elsevier, Saint Louis, pp. 315–329.
Fullenkamp, A.M., Campbell, B.M., Laurent, C.M., Lane, A.P., 2015. The contribution of trunk axial kinematics to post-strike ball velocity during maximal instep soccer kicking. J. Appl. Biomech. 31 (5), 370–376.
Graci, V., Van Dillen, L.R., Salsich, G.B., 2012. Gender differences in trunk, pelvis, and lower limb kinematics during a single leg squat. Gait Post. 36 (3), 461–466.
Hanavan, E.P., 1964. A Mathematical Model of the Human Body (AMRL-TR-64-102). Wright-Patterson Air Force Base, Ohio, pp. 1–149.
Iino, Y., Kojima, T., 2012. Validity of the top-down approach of inverse dynamics analysis in fast and large rotational trunk movements. J. Appl. Biomech. 28, 420–430.
Kellis, E., Katis, A., 2007. Biomechanical characteristics and determinants of instep soccer kick. J. Sports Sci. Med. 6, 154–165.
Lees, A., Asai, T., Andersen, T.B., Nunome, H., Sterzing, T., 2010a. The biomechanics of kicking in soccer: A review. J. Sports Sci. 28 (8), 805–817.
Lees, A., Barton, G., Robinson, M., 2010b. The influence of Cardan rotation sequence on angular orientation data for the lower limb in the soccer kick. J. Sports Sci. 28 (4), 445–450.
Lees, A., Rahnama, N., 2013. Variability and typical error in the kinematics and kinetics of the maximal instep kick in soccer. Sports Biomech. 12 (3), 283–292.
McGibbon, C.A., Krebs, D.E., 2001. Age-related changes in lower trunk coordination and energy transfer during gait. J. Neurophysiol. 85 (5), 1923–1931.
McGibbon, C.A., Krebs, D.E., Puniello, M.S., 2001. Mechanical energy analysis identifies compensatory strategies in disabled elders' gait. J. Biomech. 34 (4), 481–490.
Novak, A.C., Li, Q., Yang, S., Brouwer, B., 2011. Mechanical energy transfers across lower limb segments during stair ascent and descent in young and healthy older adults. Gait Post. 34 (3), 384–390.
Novak, A.C., Li, Q., Yang, S., Brouwer, B., 2015. Energy flow analysis of the lower extremity during gait in persons with chronic stroke. Gait Post. 41 (2), 580–585.
Nunome, H., Asai, T., Ikegami, Y., Sakurai, S., 2002. Three-dimensional kinetic analysis of side-foot and instep soccer kicks. Med. Sci. Sports Exerc. 34 (12), 2028–2036.
Nunome, H., Lake, M., Georgakis, A., Stergioulas, L.K., 2006. Impact phase kinematics of instep kicking in soccer. J. Sports Sci. 24 (1), 11–22.
Prieske, O., Muehlbauer, T., Borde, R., Gube, M., Bruhn, S., et al., 2016. Neuromuscular and athletic performance following core strength training in elite youth soccer: role of instability. Scand. J. Med. Sci. Sports 26 (1), 48–56.
Putnam, C.A., 1991. A segment interaction analysis of proximal-to-distal sequential segment motion patterns. Med. Sci. Sports Exerc. 23 (1), 130–141.
Rahnama, N., Reilly, T., Lees, A., 2002. Injury risk associated with playing actions during competitive soccer. Br. J. Sports Med., 354–359
Robertson, D.G.E., Mosher, R.E., 1985. Work and power of the leg muscles in soccer kicking. In: Winter, D.A., Norman, R.W., Wells, R.P. (Eds.), Biomechanics IX-B. Human Kinetics Publishers, Champaign, pp. 533–538.
Robertson, D.G., Caldwell, G.E., Hamill, J., Kamen, G., Whittlesey, S.N., 2014. Research Methods in Biomechanics. Human Kinetics, Champaign, pp. 1–440.
Robertson, D.G., Winter, D.A., 1980. Mechanical energy generation, absorption and transfer amongst segments during walking. J. Biomech. 13 (10), 845–854.
Serner, A., Tol, J.L., Jomaah, N., Weir, A., Whiteley, R., Thorborg, K., et al., 2015. Diagnosis of Acute Groin Injuries: A Prospective Study of 110 Athletes. American J. Sports Med. 43 (8), 1857–1864.
Shan, G., Westerhoff, P., 2005. Full-body kinematic characteristics of the maximal instep soccer kick by male soccer players and parameters related to kick quality. Sports Biomech. 4 (1), 59–72.
Sinclair, J., Fewtrell, D., Taylor, P.J., Bottoms, L., Atkins, S., Hobbs, S.J., 2014. Three-dimensional kinematic correlates of ball velocity during maximal instep soccer kicking in males. European J. Sport Sci. 14 (08), 799–805.
Tojima, M., Torii, S., 2018. Difference in kick motion of adolescent soccer players in presence and absence of low back pain. Gait Post. 59, 89–92.
V3D Composite Pelvis. In: C-Motion Visual 3D Wiki Documentation. C-Motion Inc. 2016. http://www.cmotion.com/v3dwiki/index.php?title=V3D_Composite_Pelvis. Accessed October 16, 2016.
van der Krug, E., van der Helm, F.C.T., Veeger, H.E.J., Schwab, A.L., 2018. Power in sports: A literature review on the application, assumptions, and terminology of mechanical power in sport research. J. Biomech. 79, 1–14.
Winter, D.A., 2009. Biomechanics and Motor Control of Human Movement. John Wiley & Sons Inc, Hoboken, pp. 1–325.
Zajac, F.E., Neptune, R.R., Kautz, S.A., 2002. Biomechanics and muscle coordination of human walking. Part I: introduction to concepts, power transfer, dynamics and simulations. Gait Post. 16 (3), 215–232.